frontiers | Frontiers in Earth Science

ORIGINAL RESEARCH
published: 23 May 2022
doi: 10.3389/feart.2022.895941

Study on Organic Matter Enrichment and Reservoir Characteristics of Permian Longtan Formation Shale in Southeast Sichuan

Qian Cao[1,2,3,4], *Minghui Qi*[1,3,4], *Xiawei Li*[1,3,4]*, *Daifu Wang*[1,3,4], *Yuwei Deng*[1,3,4] and *Chongyu Wu*[1,3,4]

[1]Shale Gas Evaluation and Exploitation Key Laboratory of Sichuan Province, Chengdu, China, [2]State Key of Oil and Gas Reservoir Geology and Exploitation, Chengdu University of Technology, Chengdu, China, [3]Technology Innovation Center of Shale Gas Exploration and Development in Complex Structural Areas, Ministry of Natural Resources, Chengdu, China, [4]Sichuan Keyuan Testing Center of Engineering Technology, Chengdu, China

The study of reservoir space development characteristics and the geochemical parameters of the Permian Longtan Formation in the southeast of the Sichuan Basin at Well X1 was analyzed by using core observations, optical thin-section observations, Ar-ion polishing, scanning electron microscopy, and nitrogen adsorption tests. Major and trace elements of samples, the V/Cr, U/T, enrichment coefficients EF (Mo) and EF (U), chemical alteration indexes CIA and Sr/Cu, and Mo, P, and other index values of different samples were calculated based on the test of organic geochemical parameters. The depositional environment of the Longtan Formation in the study area was systematically analyzed. The Longtan Formation was in a warm and humid climate during the deposition period. The main body of the sedimentary water was in an oxygen-depleted state, and a portion of it was in an oxidized state with high biological productivity. Therefore, it had a small deposition rate. The clay mineral content and organic matter content in the sample played a major role in controlling the development of reservoir space. The content of clay minerals in the sample was high, and it was mainly chlorite and a mixed layer of illite/smectite. Under a microscope, it was observed that the mixed layer of flake illite/smectite and chlorite aggregate mostly developed interlayer pores or microfractures, which played a positive role in the specific surface area and pore volume of the sample.

Keywords: pore development characteristics, organic matter enrichment, Longtan Formation, Southeast of the Sichuan Basin, major and trace elements of samples

OPEN ACCESS

Edited by:
Kun Zhang,
Southwest Petroleum University, China

Reviewed by:
Shengqiang Zeng,
Chengdu Center of China Geological Survey, China
Yidong Cai,
China University of Geosciences, China
Yongsheng Tan,
Institute of Rock and Soil Mechanics (CAS), China

***Correspondence:**
Xiawei Li
lxw_2020@126.com

Specialty section:
This article was submitted to Geochemistry, a section of the journal Frontiers in Earth Science

Received: *14 March 2022*
Accepted: *20 April 2022*
Published: *23 May 2022*

Citation:
Cao Q, Qi M, Li X, Wang D, Deng Y and Wu C (2022) Study on Organic Matter Enrichment and Reservoir Characteristics of Permian Longtan Formation Shale in Southeast Sichuan. Front. Earth Sci. 10:895941. doi: 10.3389/feart.2022.895941

1 INTRODUCTION

The enrichment of organic matter in shale is a complex physicochemical process. Different sedimentary environments have different productivity and preservation conditions (Arthur and Sageman, 1994; Wei et al., 2012; Pedersen and Calvert, 1990). Through the study of black organic-rich shale in marine strata, researchers around the world found that the enrichment of organic matter is the result of multi-factor coupling control (Zhang et al., 2020a). Some scholars believe that the factors affecting the preservation of organic matter, such as redox conditions, deposition rate, and water depth change at the bottom of sedimentary water bodies control the enrichment of organic matter (Demaison and Moore, 1980) (i.e., they control the "preservation mode"). Others believe that

paleoclimate, paleoproductivity, and terrestrial organic matter supply, which directly affect the input of organic matter, are the leading factors (Wignall and Newton, 2001) that control the "production mode." The content of total organic carbon (TOC) in sediments is affected by organic matter input and preservation capacity. For the input of organic matter, the more the sources of organic matter, the higher the input and the higher the content of TOC in sediments.

In the process of multi-cycle tectonic evolution and sedimentation, many sets of organic-rich shale strata of marine, continental-marine, and continental sediments have been developed in China (Zhao et al., 2020; Zhang et al., 2022a; Zhang et al., 2022b). Among them, there are abundant shale gas resources in continental-marine transitional facies, with a resource amount of about $19.8\% \times 10^{12}$ m^3, accounting for 25% of China's total shale gas resources. Therefore, they have great exploration and development potential (Dong et al., 2016). The Permian in the Sichuan Basin was in the Paleo-Neo-Tethys transformation period, which produced a series of geological events and changes in the sea level. During the deposition of the Longtan Formation, affected by the uplift of the Emei mantle plume and the movement of the Emei ground fissure (two prototype basins), a stable craton basin and an extensional rift deeper-water basin were formed in the Sichuan Basin and its periphery, with extremely rich sedimentary systems and facies belt types. From the southwest to the northeast, the sedimentary facies changes from marine-land transitional facies to shallow marine continental shelf facies (He et al., 2021a; Wei et al., 2015; Chen et al., 2020). The continental-marine transitional facies shale of the Permian Longtan Formation in the southeast of Sichuan has a thin single layer and a large cumulative thickness. Multiple sets of coal seams/coal lines are developed, showing the characteristics of frequent interbedding of shale, coal seam, sandstone, and limestone (He et al., 2021a). Compared with the marine sedimentary shale of the Longmaxi Formation, the continental-marine transitional facies shale of the Longtan Formation has different organic matter content and types in the delta facies and lagoon tidal flat facies affected by marine and terrigenous rivers, and there are also great differences in reservoir performance. Thus, it is imperative to research the enrichment law of shale organic matter and reservoir performance in the study area.

At present, scholars in China and abroad have used a combination of core observation, whole-rock X-ray diffraction analysis, thin section identification, light sheet identification, organic geochemistry, inorganic geochemistry, and other tests in the study of the distribution of organic matter. Furthermore, the mineral assemblage characteristics of sedimentary rocks and the distribution characteristics of organic matter maturity and source are evaluated, and the comprehensive influencing factors of organic matter distribution are further analyzed (Liu et al., 2007; Yin et al., 2017; Hatch and Levanthal, 1992; Tribovillard et al., 2012a; Tribovillard et al., 2012b). Based on the petrological characteristics, organic geochemical characteristics, and reservoir spatial distribution characteristics of different samples in the study area, the dynamic response relationship among paleoclimate, redox environment, paleoproductivity, siderite, and other mineral distributions with different organic matter enrichment was further analyzed in this study. Moreover, the enrichment law of organic matter was clarified in continental-marine transitional facies shale in the study area, and the spatial development characteristics and main controlling factors of the shale reservoir were analyzed.

2 GEOLOGICAL SETTINGS

After the deposition of the Middle Permian, due to the influence of the Soochow movement, the sea water retreated eastward, resulting in the rise of the western part of the Sichuan Basin onto the land. Thus, the paleogeographic pattern of "west land and East China Sea," which is high in the southwest and low in the northeast, was formed. In the early Late Permian, the distribution of sedimentary facies in the basin showed an obvious evolution from continental facies to marine facies from the west to the east. Because of the differences in the paleogeographical pattern and sedimentary environment, the characteristics of different facies in the same period are obvious. The sedimentary facies belt of the whole Sichuan Basin is from the southwest to the northeast in order from basalt eruption area- river and lacustrine facies- shore/swamp facies- tidal flat/lagoon facies- platform facies- slope/shelf facies- shelf facies. It is distributed in an arc-shaped belt (**Figure 1A**), with diverse sedimentary rock types and complex rock assemblages. The Longtan Formation in the southern Sichuan Basin is a series of widely deposited coal-bearing rocks with a thickness of 20–120 m in parallel unconformable contact with the Maokou Formation. From land to sea, the sedimentary facies belt spreads roughly in a west-to-east direction and extends in a north-to-south direction and mainly develops a tidal flat-lagoon sedimentary system (Zhang et al., 2015; Zhang et al., 2014; Guo et al., 2018; Cheng et al., 2020). The water is shallow, with a warm and humid tropical rainforest climate, and the development of peat swamps helps the growth, deposition, and preservation of terrestrial plants, making it ideal for the enrichment of organic matter.

3 SAMPLES AND METHODOLOGY

Fifteen samples were taken from Well X1 at the southeastern margin of the Sichuan Basin (**Figure 1A**), located in the low-steep fold belt. The lithology of the Longtan Formation is mostly black shale and carbonaceous shale, with developing coal seams (He et al., 2021a; **Figure 1B**).

TOC content was measured using an RJXWK-1 carbon-sulfur analyzer according to the TOC test standard for sedimentary rocks (GB/T 19145-2003). The thermal evolution maturity (Ro) of the organic matter was measured using a Zeiss Axio Scope A1 polarized light microscope and a TIDAS S MSP 400 spectrophotometer (J&M Analytik AG) in line with the standard vitrinite reflectance test procedure for sedimentary rocks (SY/T 5124-2012). Organic matter types were determined using a Zeiss Axio Scope A1 polarized light microscope, in agreement with the standard method of

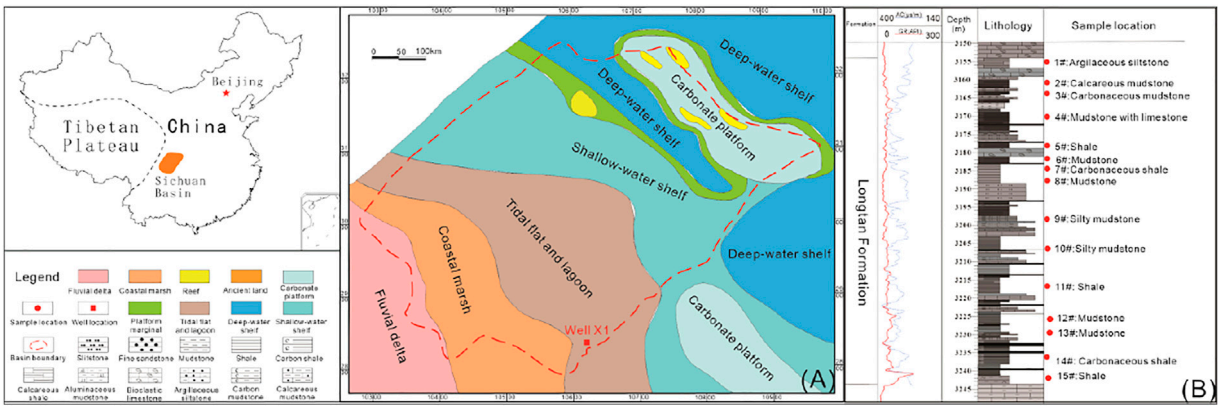

FIGURE 1 | Geographical location, sampling location, and stratigraphic description of the Longtan Formation in the study area. **(A)** Sample location; **(B)** Well X1 in the Longtan Formation and modified from references [Nesbitt and Young (1982) and Huang et al. (2021)].

kerogen maceral identification and classification (SY/T 5125-2014). The macerals, morphology, and structure of kerogen were observed under transmitted light and fluorescence. Because the kerogen extraction process may destroy the structure of organic matter and the developmental state of some organic matter in shale, and thus, may affect the determination of the source of the organic matter, the samples were observed in thin sections.

A qualitative analysis of the mineral composition was conducted using a Zeiss Axio Scope A1 polarized light microscope according to the SY/T 5368-2016 thin-section identification standard. A quantitative analysis of mineral composition was carried out on an X'Pert Powder X-ray diffractometer (Malvern Panalytical), in agreement with the standard XRD analysis method for clay and common non-clay minerals in sedimentary rocks (SY/T 5163-2010).

SEM test was performed on a Zeiss Sigma 300 scanning electron microscope in line with the standard SEM procedure for rock samples (SY/T5162-2014), and the images were analyzed using image analysis software (Image-pro Plus) to determine the pore structure parameters (i.e., the number, diameter, width, perimeter, and area).

The nitrogen adsorption test was used to determine the specific surface and pore size distribution of the rock using the static nitrogen adsorption volume method (Micrometrics ASAP 2460 automatic specific surface and pore size analyzer) to complete the test process according to GB/T 19587-2017/ISO 9277: 2010.

The content of major elements was determined using an Axios mAX X-ray fluorescence spectrometer (Malvern Panalytical) in agreement with the GB/T 14506.28-2010 standard. Testing accuracy was determined to be better than ±3%.

4 RESULTS

This section is divided into several subheadings. The section provides a concise and precise description of the experimental results, their interpretations, and the conclusions that can be drawn from the experiments.

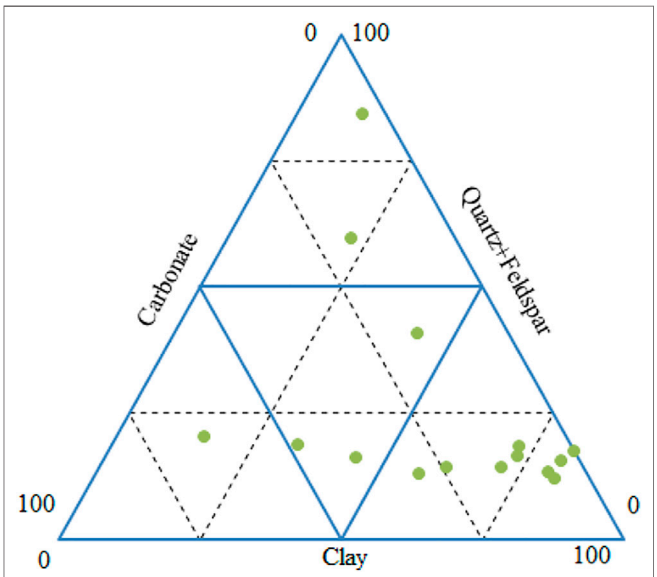

FIGURE 2 | Distribution of mineral component content of samples in the study area.

4.1 Lithology and Sedimentary Characteristics

The Permian Longtan Formation in the study area is a set of coal-bearing carbonaceous shale with continental-marine transitional facies. The Longtan Formation has roughly experienced the process of hydrostatic low energy, medium-low energy, and low energy from the bottom to the top (He et al., 2021b; Wang et al., 2020). The horizontal distribution of the Longtan Formation in the southeast of Sichuan is stable, and the stratum thickness is

TABLE 1 | Types of kerogen and reflectance of Longtan Formation samples.

Samples	Lithology	Depth (m)	TOC (%)	Maceral identification and type					R_{ran} (%)				
				Exinite %	Vitrinite %	Inertinite %	Type index	Type	Minimum	Maximum	Mean	Standard deviation	Measuring points
1#	Limestone	3,157.80	5.85	78	14	8	20.5	II_2	2.23	2.55	2.39	0.08	20
2#	Lime mudstone	3,159.32	3.44	66	28	6	6	II_2	3.05	3.43	3.11	0.11	20
3#	Carbonaceous mudstone	3,161.23	3.38	62	33	5	1.25	II_2	2.22	2.61	2.4	0.11	20
4#	Lime-bearing mud layer	3,163.20	1.35	42	53	5	–23.75	III	2.47	2.86	2.65	0.11	20
5#	Lime-bearing mud layer	3,165.31	1.21	76	19	5	18.8	II_2	2.38	2.83	2.62	0.13	20
6#	Mudstone	3,167.37	4.37	54	41	5	–8.75	III	2.52	2.85	2.69	0.09	20
7#	Silty mudstone	3,168.80	5.07	80	17	3	24.3	II_2	2.97	3.42	3.23	0.13	16
8#	Mudstone	3,171.77	3.98	23	71	6	–47.75	III	2.96	3.41	3.26	0.11	20
9#	Mudstone	3173.48	1.98	65	23	12	3.3	II_2	3.06	3.48	3.32	0.12	15
10#	Silty mudstone	3,175.20	1.96	64	32	4	4	II_2	3.14	3.56	3.43	0.12	12
11#	Carbonaceous mudstone	3,177.12	1.28	30	65	5	–38.75	III	3.21	3.57	3.45	0.11	10
12#	Mud shale	3,180.18	0.23	38	55	7	–29.3	III	3.23	3.55	3.49	0.12	10
13#	Muddy siltstone	3,182.39	3.15	66	30	4	6.5	II_2	3.11	3.56	3.53	0.12	15
14#	Shale	3,185.04	0.61	74	24	2	17	II_2	3.29	3.72	3.55	0.13	20
15#	Silt-bearing mudstone	3,186.71	2.95	82	16	2	27	II_2	3.35	3.75	3.57	0.12	16

between 70–80 m. There are great differences in the horizontal distribution of different lithologic thicknesses (He et al., 2021a; Guo et al., 2018; Cheng et al., 2020; Yang et al., 2021). According to the whole rock test results of X-ray diffraction, the mineral components of the sample are mainly clay minerals, with a clay content of 8%–79% and an average clay content of 48.46%, followed by clastic components such as quartz, with a content of 6%–55% and an average content of 18%. Carbonate minerals are mainly dolomite and calcite, with a content of 10%–59% and an average content of 18.5% (**Figure 2**). According to the thin section identification results, the lithology of the Longtan Formation in the study area is chiefly lithic sandstone, mudstone, siderite, and a small amount of carbonate rock (e.g., bioclastic limestone, mud silty dolomite, and siderite). It can be observed that the coal seam/coal line is developed, and the bioclastic rocks mainly include bryozoan, foraminifera, and a small amount of brachiopod and bivalve fragments (**Figure 2**).

4.2 Organic Geochemical Characteristics of Shale Reservoir

The type of organic matter not only determines the hydrocarbon generation capacity of source rocks and the properties of generated hydrocarbons, which affects the occurrence and migration of gas in shale, but also affects the development of different types of reservoir spaces. The microscopic component type of organic matter is determined by the microscopic fractal characteristics obtained using a polarizing microscope. The analysis results of the organic matter type of the test sample of the Longtan Formation are shown in **Table 1**. The results show that the kerogen types of the Longtan Formation in the study area are type II_2 and type III. The main macerals are exinite and vitrinite, with an average content of 60.00% and 36.73%, respectively. This shows that the organic matter primarily comes from the fragments of reproductive organs and epidermal tissues of terrestrial higher plants. After strong degradation, the organic matter finally displays the distribution of debris or part of cotton wadding, and occasionally, some vitrinite is attached with humic amorphous minerals around. Different lithologies have certain differences in the types of organic matter. The micro-component structures of different shale samples observed under a polarized light microscope are largely primary structures, massive structures, and fine plant debris that is scattered. Vitrinites with woody structures are often found in coal and rock samples, and they are mostly distributed in strips or blocks. They are suspected to be formed by the humic degradation of plant stems, leaves, wood fibers, or some marine plants (**Figure 3**). The test results of the organic matter content and vitrinite emissivity of the samples indicated that the organic matter content of the Longtan Formation mud shale samples has a wide distribution range, ranging from 0.5% to 5.2%, mainly from 2.0% to 3.0% and 4.0% to 5.0% (**Table 2**). The maturity distribution is not very different, with Ro ranging from 2.39% to 3.57%, with an average value of 3.11% (**Table 2**), all of which are in the high maturity stage.

The organic matter in the mud shale of the Longtan Formation can be divided into dispersed isolated organic matter and symbiotic organic matter observed by optical microscopy and high-resolution scanning electron microscopy. The isolated organic matter is predominantly in the form of agglomerates,

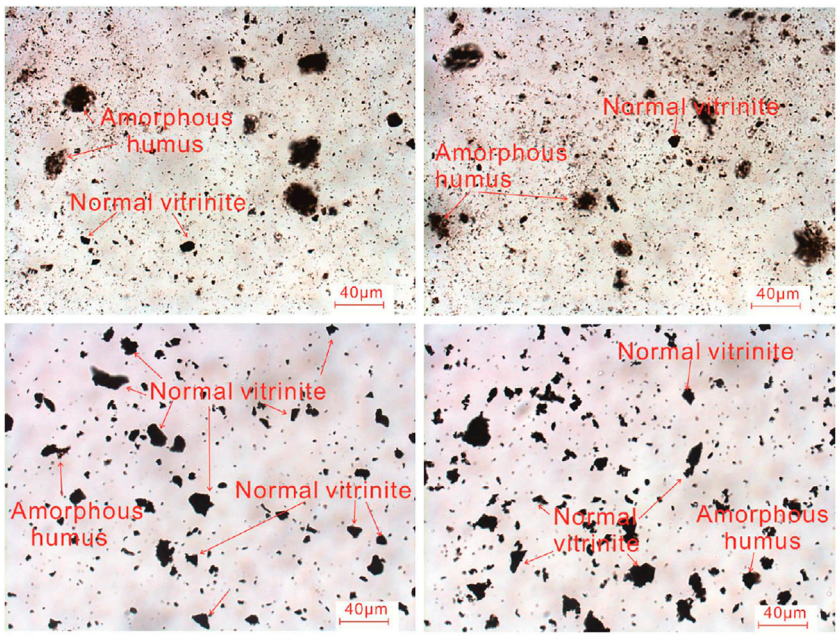

FIGURE 3 | Light sheet fluorescence photos of typical samples of Longtan Formation shale.

TABLE 2 | Major element oxide contents of different Longtan Formation samples in the study area (%).

Samples	Major element content (%)										Loss on ignition (%)	CIA (g/mol)	P (μg/g)	P/Al
	SiO_2	Al_2O_3	MgO	Na_2O	K_2O	P_2O_5	TiO_2	CaO	TFe_2O_3	MnO				
Detection limit	0.0335	0.0375	0.0277	0.0021	0.0382	0.0019	0.0333	0.0438	0.0078	0.0138	/	/	/	/
1#	40.51	13.47	2.26	0.52	1.84	0.17	2.6	11.52	8.02	0.1	18.34	84.01	742.254	0.010
2#	33.57	14.16	2.89	0.74	0.91	0.31	2.83	7.73	15.89	0.15	18.01	82.6	1353.521	0.018
3#	42.62	24.25	0.83	1.07	1.34	0.33	4.57	0.7	6.6	0.02	17.37	84.86	1440.845	0.011
4#	38.04	23.34	1.02	1.1	0.9	0.21	5.08	0.75	12.43	0.17	16.62	83.78	916.901	0.007
5#	43.35	24.07	1.33	1.1	0.96	0.36	4.57	1.58	7.53	0.06	14.22	80.87	1571.831	0.012
6#	40.3	23.19	1.15	1.45	1.4	0.4	4.79	0.86	9.58	0.11	16.32	81.94	1746.479	0.014
7#	41.71	15.07	3.43	0.63	0.48	0.37	4.2	5.46	16.22	0.09	9.81	87.2	1615.493	0.020
8#	35.27	10.01	3.83	0.15	0.2	0.43	1.7	11.8	19.84	0.16	15	81.72	1877.465	0.035
9#	40.64	19.15	2.12	1.38	1.32	0.42	3.11	4.12	11.9	0.16	14.8	83.56	1833.803	0.018
10#	36.34	12.73	2.61	0.59	0.52	0.18	1.59	1.08	28.45	0.3	15.81	87.85	785.915	0.012
11#	40.92	19.39	1.74	1.14	1.63	0.41	3.66	2.48	12.28	0.16	15.44	79.9	1790.141	0.017
12#	38.92	23.07	1.09	0.87	1.97	0.06	4.1	0.62	14.45	0.04	14.47	82.84	261.972	0.002
13#	39.58	22.98	0.66	1.17	1.46	0.21	3.78	0.69	10.15	0.2	19.53	82.69	916.901	0.008
14#	41.36	25.39	0.47	0.62	0.83	0.23	4.55	0.5	6.06	0.11	20.11	79	1004.225	0.007
15#	37.94	19.62	1.35	0.59	3.02	0.45	3.36	3.51	14.37	0.15	13.11	86.1	1964.789	0.019

strips, or fragments and is independently scattered in the matrix. Some of them are distributed in a curved shape parallel to the bedding direction, with obvious structural features. Most of them are closely combined with the mineral matrix and have clear boundaries (**Figure 4J**). The distribution of symbiotic organic matter is primarily irregular, such as banded and interstitial distribution, and co-grown with matrix minerals around the organic matter, filling the gap between inorganic mineral particles/crystals such as siliceous minerals, clay minerals, and pyrite. Its boundaries are mainly mixed with the boundaries between mineral grains/crystals (**Figures 4K,L**).

4.3 Distribution of Major, Trace, and Rare Earth Elements in Shale Reservoirs

The geochemical characteristics of trace elements are not only related to the properties of the elements themselves but are also affected by various external environments. Therefore, in different sedimentary environments, the laws of element dispersion and aggregation are also different, which provides a theoretical basis for paleoenvironmental analysis using trace elements and their contents in sediments. In this study, 15 samples of the Longtan Formation were tested for major, trace, and rare earth elements to analyze the sedimentary environment of the study area and then

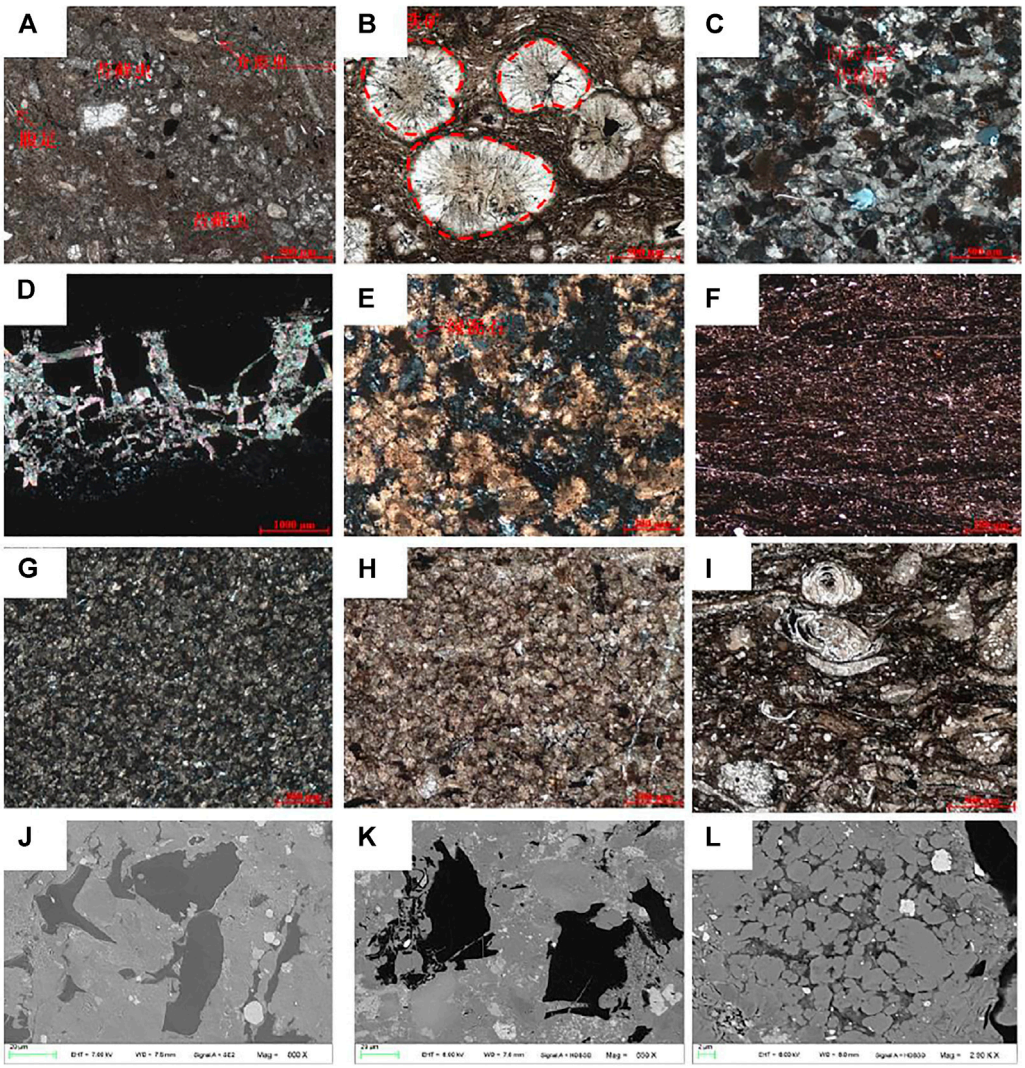

FIGURE 4 | Thin section identification and SEM observation results of the Longtan Formation reservoir in well X1. **(A)** Micritic dolomite containing bioclastic. **(B)** Siderite mudstone and siderite in a nodular and spherical shape, with radial structure inside. **(C)** Dolomitic fine-grained lithic sandstone, with rock debris mostly replaced by dolomite. **(D)** Coal rock, with cracks filled with calcite. **(E)** Siderite rock, radial, with chlorite at the core. **(F)** Mudstone. **(G)** Dolomitic siderite rock, with siderite predominantly composed of fine microcrystalline granular aggregates; the whole body is granular and lumpy, mainly in the form of metasomatic dolomite minerals. **(H)** Fine powdery siderite rock, mainly composed of siderite, light yellowish brown as a whole, mostly in semi-idiomorphic granular form. **(I)** Argillaceous clastic limestone; some bryozoans are tubular and branched, and a few foraminifera are spindle-shaped, which are metasomatized by calcite and silica. **(J)** Fragmented and banded organic matter is distributed intensively. **(K)** The gap between each mineral component and the crushed massive organic matter are in close contact with the surrounding mineral components. **(L)** Microcrystalline quartz (siliceous), clay minerals, and organic matter coexist with each other.

to study the factors affecting the distribution of organic matter in the Longtan Formation. The test results are shown in **Tables 2**, **3**.

4.4 Development Characteristics of Reservoir Space

4.4.1 Pore Type

Ar-ion polishing and field-emission SEM were utilized to observe the development characteristics of the microscopic storage space in samples from the Longtan Formation in the study area. Based on the pore-type classification of organic-rich shale (Cao et al., 2015; Zhang et al., 2022c; Zhang et al., 2020b) and the genetic and structural characteristics of shale pores, the main storage space of marine-continental transitional shale in the Longtan Formation was identified to consist of inorganic pores, organic pores, and microfractures. Inorganic pores are predominantly distributed between clay mineral particles or in detrital particles such as quartz. Clay minerals with unstable chemical properties will generate a large number of pores during the process of sedimentary burial and will transform into a mixed layer of illite/smectite and illite. It can be seen that interlayer pores and fractures are abundantly developed in the lamellar illite/

TABLE 3 | | Trace element contents, rare earth element contents, and related parameters of mud shale samples from the Longtan Formation.

Samples	Trace element content (ug/g)									Element ratio				
	V	Cr	Co	Ni	Cu	Sr	Mo	Ba	U	Sr/Cu	U/Th	V/Cr	EFMo	EFu
1#	295.14	201.24	51.64	103.89	123.49	705.84	5.42	307.99	9.47	5.72	0.93	1.47	4.95	3.74
2#	118.53	28.86	67.82	192.33	72.75	253.92	2.94	40.64	1.42	3.49	0.31	4.11	10.41	2.18
3#	71.31	50.28	10.96	63.03	80.16	239.02	0.89	72.09	0.85	2.98	0.34	1.42	2.79	1.16
4#	324.71	162.97	47.64	51.21	211.99	628.83	0.81	291.41	2.69	2.97	0.22	1.99	0.45	0.65
5#	171.02	53.93	50.27	51.15	126.96	341.13	0.73	162.56	2.95	2.69	0.27	3.17	0.75	1.32
6#	54.70	53.96	4.54	20.13	44.54	244.96	1.39	762.65	3.39	5.50	0.38	1.01	2.35	2.49
7#	34.02	23.78	39.43	89.13	28.02	127.01	0.74	34.16	1.16	4.53	0.36	1.43	3.18	2.16
8#	577.89	791.70	18.82	113.50	99.51	167.02	0.33	45.23	4.37	1.68	0.18	0.73	1.18	0.73
9#	359.17	171.69	57.02	113.78	232.22	739.61	1.78	488.48	3.00	3.18	0.22	2.09	0.99	0.72
10#	685.76	1100.56	11.70	96.62	26.91	122.91	0.37	42.21	5.69	4.57	0.16	0.62	0.65	0.94
11#	100.97	62.28	48.86	83.42	85.59	253.98	0.88	104.99	1.30	2.97	0.26	1.62	0.64	2.51
12#	181.60	139.74	22.18	106.53	75.82	87.84	1.08	243.44	1.33	1.16	0.28	1.30	0.48	1.48
13#	320.96	111.54	41.82	65.00	188.32	627.73	1.14	315.37	4.44	3.33	0.26	2.88	0.55	1.27
14#	171.43	70.35	63.06	177.79	124.90	299.27	1.04	91.17	2.96	2.40	0.23	2.44	0.66	1.37
15#	152.65	160.18	23.49	42.71	36.40	193.87	1.81	169.63	2.27	5.33	0.58	0.95	0.83	1.41

Samples	Rare earth element content (ug/g)						$(La/Yb)_N$
	La	Yb	Sc	Y	Tb	Th	
1#	65.58	4.12	27.06	42.65	1.58	10.22	10.723
2#	389.09	17.25	11.41	370.10	9.38	4.54	15.204
3#	20.64	3.44	14.34	48.34	1.69	2.49	4.042
4#	86.05	5.47	31.10	59.42	2.02	12.17	10.608
5#	82.37	4.71	17.99	54.42	1.96	11.05	11.786
6#	48.55	2.68	6.54	31.91	0.97	8.92	12.213
7#	17.94	1.61	5.05	22.70	0.80	3.23	7.533
8#	131.68	8.59	38.02	75.96	2.66	24.63	10.340
9#	82.87	4.94	37.75	60.31	2.35	13.55	11.306
10#	133.88	16.02	36.46	95.67	3.94	34.58	5.636
11#	33.38	2.16	12.04	24.08	1.01	4.98	10.421
12#	31.26	2.33	7.97	25.82	0.83	4.73	9.037
13#	166.17	5.93	27.26	61.42	2.05	17.10	18.885
14#	85.17	7.22	20.38	75.71	2.23	13.05	7.950
15#	26.32	1.46	11.68	17.21	0.67	3.94	12.187

smectite mixed-layer aggregates that are distributed in a curved and irregular shape (**Figures 5A–C**). These interlayer and intralayer micropores not only create space for the occurrence of shale gas but also provide microscopic migration channels for gas seepage. Some minerals such as quartz and pyrite are disturbed by the external environment during the growth process, resulting in the formation of intracrystalline pores during the crystal accumulation process (**Figures 5D,E**). The pore size varies from a few nanometers to several hundred nanometers. The degree of development of pores is low, and their connectivity is poor. Occasionally, because of the dissolution of mineral crystals such as siderite, certain intergranular (grain) dissolution pores will also be formed on the edges (**Figure 5F**). These intergranular dissolved pores are often harbor-shaped or elongated. Few dissolved pores were observed under a microscope in the samples of the study area.

Under the microscope, the organic matter in the test samples of the Longtan Formation was primarily distributed in isolated shapes, such as fragments or strips, with obvious structural features, suspected plant fragments, and other animal and plant fabrics which were mainly closely combined with the mineral matrix and had clear boundaries. Zooming in on the development of pores in this type of organic matter showed that there were various shapes, including round, oval, flat, elongated, and irregular. The pores were almost undeveloped and had poor connectivity (**Figures 5G–J**). We can also observe that some organic matter grows together with surrounding matrix minerals (clay, quartz, calcite, and other minerals) in the form of interstitials. Furthermore, their boundaries are mostly mixed with the boundaries between mineral particles/crystals, and a large number of pores can be seen in the interior and edges of this type of organic matter. The pore shape is largely circular and oval. Some pores have good connectivity with a wide range of pore size distribution (**Figures 5K,L**). Microfractures are chiefly developed between crystals or within clay mineral particles, and a small amount is also distributed on the edge of organic matter. They are principally exogenous cracks and inter-particle cracks formed under the action of external force, and the crack width is generally 1–20 μm. Some microfractures cut straight through detrital grains or clay mineral grains. It can also be observed that certain shrinkage pores and seams develop between organic matter and mineral particles (**Figure 5I**), which is primarily due to the volume shrinkage during the thermal evolution of organic matter. The results demonstrated that the dominant storage spaces in different test samples were the pores

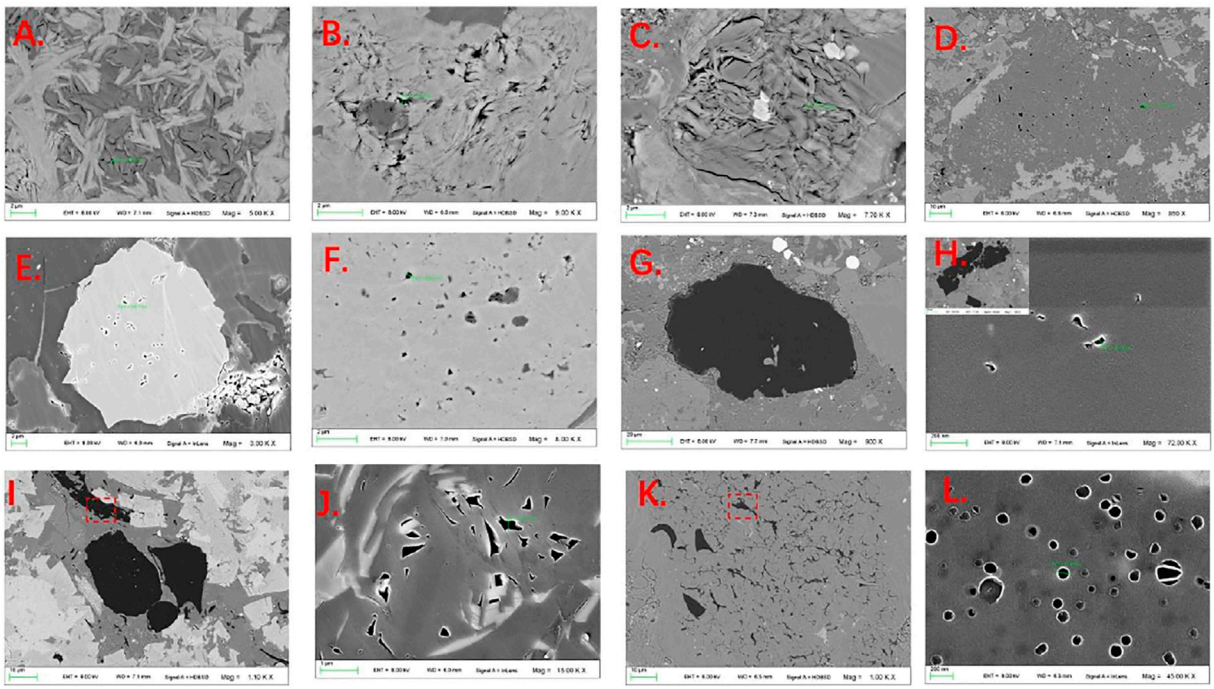

FIGURE 5 | Spatial distribution characteristics of microscopic reservoirs in different shale samples of the Longtan Formation. **(A)** The interlayer pores and fractures are developed in the lamellar smectite mixed layer and chlorite aggregates (×5000). **(B)** The interlayer pores and fractures are developed in the lamellar chlorite aggregates (×9000). **(C)** Transformed from feldspar clay minerals developed from interlayer fractures (×7700). **(D)** Contiguous quartz (siliceous) developed angular dissolution pores (×850). **(E)** Strawberry-shaped pyrite developed inter-crystalline pores (×3000). **(F)** Irregular dissolution pores developed in siderite (×3500). **(G)** Angled pores developed in organic components (×15000). **(H)** Arc-shaped organic matter developed circular pores (×45000). **(I)** Microfractures developed in fragmented organic matter (×40000). **(J)** Enlarged observation of interstitial organic matter in **(G)**; round pores (×45000) developed inside the organic matter. **(K)** Concentrated distribution of fragmented and banded organic matter (×1100). **(L)** The enlarged observation of organic matter in **(K)** shows the development of angular pores (×15000).

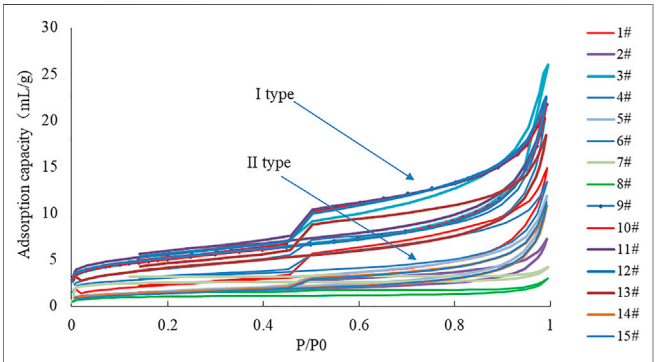

FIGURE 6 | Liquid nitrogen adsorption and desorption curves of different samples.

and fractures and microfractures between clay mineral layers, and the organic pores were less developed.

4.4.2 Development Characteristics of Pore Structures Such as Porosity, Specific Surface Area, and Pore Volume

The porosity and pore structure development characteristics of different test samples were tested using the helium gas method and the liquid nitrogen isotherm adsorption method, respectively. The hysteresis loop characteristics of liquid nitrogen adsorption–desorption curves can qualitatively reflect the morphological characteristics of pores to a certain extent. However, shale reservoirs have various pore types, and the hysteresis loop often represents the superposition of multiple typical curves. **Figure 6** exhibits the characteristics of liquid nitrogen adsorption/desorption experiments. According to IUPAC's liquid nitrogen adsorption/desorption curve classification scheme, the sample adsorption loops can be divided into two categories (IUPAC, 1982). The first type of adsorption loop has both the H2 and H3 curve characteristics of IUPAC. That is, the adsorption and desorption curves in the low-pressure section ($0 \leq P/P0 < 0.4$) overlap, and the medium-pressure section ($0.4 \leq P/P0 < 0.8$) has an obvious inflection point and a wide hysteresis loop. This indicates that the corresponding pore structure is complex, in which ink bottle–type pores are the typical pores. In the high-pressure section ($0.8 \leq P/P0 \leq 1.0$), the slopes of both adsorption and desorption curves increase, indicating that there are groove-like open pores in the larger pore size range. The second type of adsorption loop has similar characteristics to the H3 and H4 curves. The adsorption/desorption curves of the low- and medium-pressure sections almost overlap, and the inflection point is not obvious. This

suggests that the pore types in the test samples are simple, and most of them are slit-type micropores. The liquid nitrogen desorption curves of different samples were selected to calculate the pore structure parameters, in which the specific surface area was calculated using the BET model, the pore volume was calculated using the BJH model, and the fractal dimension was calculated using the FHH model. The results suggested that the porosity value of the samples was distributed between 1.27% and 6.92%, with an average value of 3.67%. The specific surface area was distributed in the range of 3.645–24.22 m^2/g, with an average value of about 11.944 m^2/g. The classification of pores in this research adopted the classification criteria recommended by IUPAC. The frequency of the specific surface area of micropores was large, indicating that the micropores were developed and played a major role in the specific surface area of the samples. The specific pore volume was mainly distributed in the range of 0.0025–0.0310 ml/g, with an average value of about 0.0177 ml/g. The mesopore volume mainly contributed to the specific pore volume of the sample, followed by macropores.

Using the nitrogen adsorption curve data of the test sample, the fractal dimension of pore distribution of different samples was calculated using the Frenkel Halsey Hill (FHH) model method. The intercept point of P/Po∈ (0.45, 0.85), ln(V), and ln [ln(Po/P)] were employed to make a curve (Zhang et al., 2018), and the corresponding curve was calculated according to the slope value of the fitted straight line. The results demonstrated that the fractal dimension distribution of different test samples was 2.37–2.91, with an average value of about 2.70, indicating that the pore distribution in the samples had strong heterogeneity.

5 DISCUSSION

5.1 Analysis of Influencing Factors of Organic Matter Enrichment

Shale organic matter enrichment is a complex physical and chemical process that involves many factors, such as the biological productivity, redox state of bottom water, deposition rate, and post-deposition degradation process (Arthur and Sageman, 1994; Wei et al., 2012). At present, after a lot of research and discussion by predecessors, it is believed that the enrichment of organic matter is mainly closely related to the preservation of a large amount of biomass, and the premise of their preservation is the prosperity of microorganisms and favorable sedimentary and burial conditions (such as hypoxia and appropriate paleoproductivity, deposition rate, etc.). Therefore, the analysis of the sedimentary environment in the study area is an important part of the study of organic matter enrichment factors.

5.1.1 Analysis of Water Oxidation Environment and Paleoproductivity

Element ratios such as V/Cr and U/Th are broadly used to indicate the redox state of water bodies. The smaller the ratio, the higher the oxidation degree of the water body. On the contrary, the larger the ratio, the stronger the reduction degree of the water body. Th is not affected by redox conditions and usually exists in the form of insoluble TH4+, while U is dissolved in water in the form of U6+ under oxidative conditions. The lower the U/Th ratio, the lower the oxygen-poor or reducing environment. The V/Cr ratio increases as the oxygen content of the water decreases. Generally, V/Cr smaller than 2.00 indicates an oxidizing environment, V/Cr greater than 4.25 shows a reducing environment, and V/Cr between 2.00 and 4.25 indicates an oxygen-poor environment. The U/Th distribution of the mud shale samples in the Longtan Formation ranged from 0.22 to 0.93, with an average value of 0.38, and the V/Cr distribution ranged from 0.62 to 4.11, with an average value of 1.82 (**Table 2**; **Figures 7**, **8**), indicating the depositional period of the organic-rich shale in the Longtan Formation. The main body of the water body is in an oxygen-depleted state, and in some periods, it is an oxidizing environment.

The enrichment factor (EF) can reflect the enrichment degree of elements in sediments. To exclude the influence of terrigenous clastic components on authigenic components, the relatively stable Al element in the diagenetic process is often used to normalize the trace elements (Tribovillard et al., 2006). To make the standardized results easy to interpret, they are generally compared with the average shale value (Wedepohl, 1971), expressed as the enrichment factor (EF), and the calculation formula is as follows:

$$EF_X = (X/A1)_i / (X/A1)_{ave}$$

When EF_X is greater than one, it indicates that element X is enriched relative to the average shale. Conversely, when EF_X is smaller than one, it indicates that element X is depleted relative to the average shale.

U and Mo are valence-variable elements that mostly exist in the form of authigenic components in sedimentary rocks. During the diagenetic process, almost no migration occurred, and the original records of the depositional period were well maintained (Zhu et al., 2010; Cai et al., 2007). When U is enriched but Mo is not, a depositional environment that may be anoxic is indicated. When they are significantly enriched at the same time, it is indicative of a sulfided depositional environment. That is, it indicates the sedimentary environment with a certain amount of H_2S in the water body (Chang et al., 2009). By calculating the enrichment coefficients of Mo and U, it can be found that most of EF (Mo) and EF (U) are distributed in the range of (0, 1) and are enriched (**Table 1**; **Figure 8**). This demonstrated that the main body of water in the study area was in an oxygen-deficient state during the deposition of organic-rich shale, and some periods were oxidative environments.

In recent years, more and more studies have confirmed that the content of Mo and P in organic-rich sediments can be employed as an indicator to measure the level of paleoproductivity. The Mo content of the mud shale of the Longtan Formation in the study area is (0.37–5.42) × 10^{-6}, with an average value of 1.49 × 10^{-6} (**Table 1**), which is larger than the corresponding value of PAAS (1.0 × 10^{-6}) (Post Archean Australian sedimentary rocks) (Taylor and McLennan, 1985). The content of P is high, ranging from 261.97 to 1964.79 ug/g with an average value of 1,321.50 μg/g. The higher the content of Mo and P, the higher the paleoproductivity of

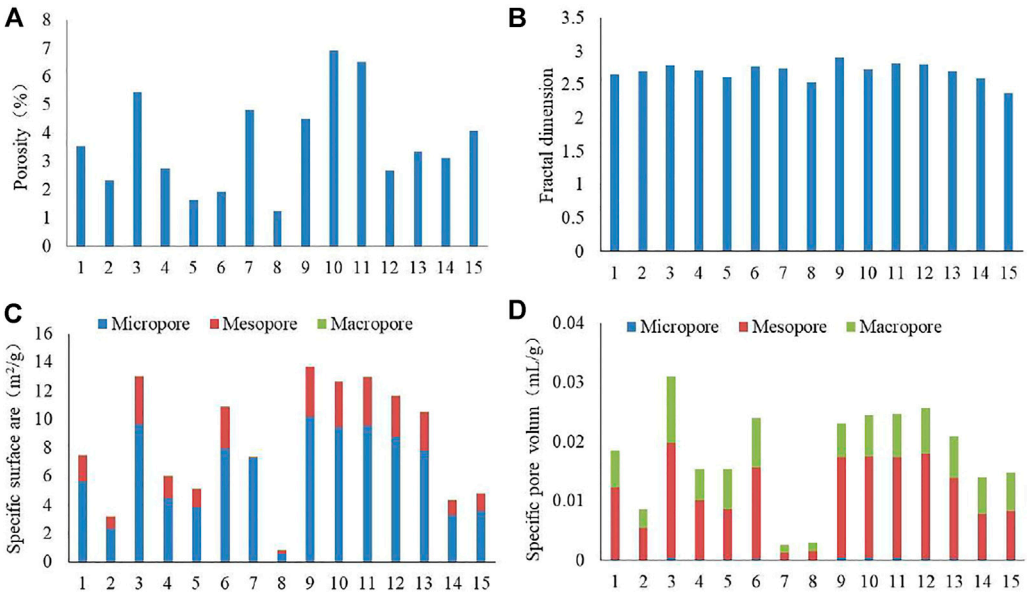

FIGURE 7 | Pore structure characteristic parameters of samples. **(A)** Porosity. **(B)** Fractal dimension. **(C)** Specific surface area. **(D)** Specific pore volume.

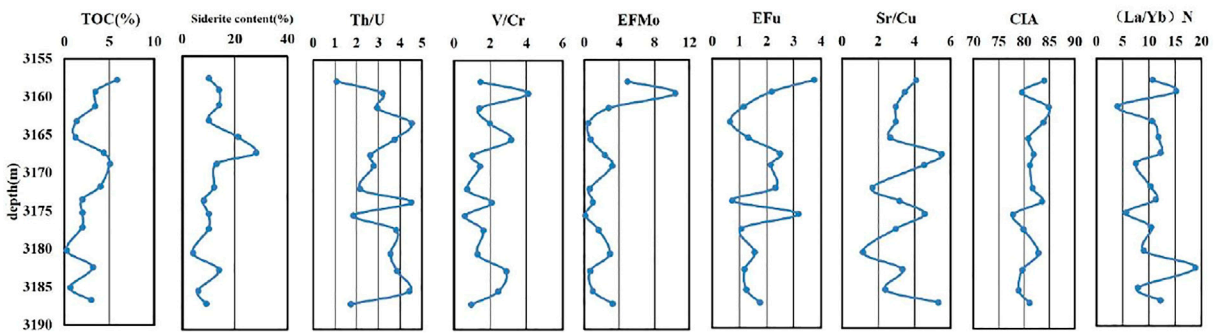

FIGURE 8 | Vertical trend of TOC, water redox indicators [Th/U, V/Cr, EF (Mo), and EF (U)], paleoproductivity indicators (Mo and P), paleoclimate indicators (CIA and Sr/Cu), and the vertical variation trend of the deposition rate index ((La/Yb)N) of Longtan Formation mud shale in Well X1.

the Longtan Formation shale during the depositional period. This is of great significance for the organic matter enrichment of the Longtan Formation transitional shale in the study area. Furthermore, the development of siderite in shale is mostly sedimentary, and its deposition often requires a weakly alkaline reducing environment. The development of siderite in the test samples was observed under a microscope, mainly in the form of $Fe(OH)_3$ colloids in the form of colloidal, microcrystalline, or spherical and radial aggregates. **Figure 8** shows that the change trend of the siderite content and the organic matter content of the test samples in the study area is consistent, which further indicates that the mud shale of the Longtan Formation in the study area was formed in a reducing environment. During the thermal evolution of organic matter in shale reservoirs of the Longtan Formation, iron oxides or hydroxides can be used as oxidants to oxidize organic matter. On the one hand, Fe^{3+} in the colloid is reduced to Fe^{2+}, and on the other hand, CO_2 can be generated and the reduced Fe^{2+} can be fixed in the form of siderite. At the same time, the thermal decarboxylation of organic matter will generate a large amount of CO_2, which can easily be combined with Fe^{2+} in the pore water to form a large number of siderite crystallites. Part of the colloidal siderite undergoes recrystallization in the later stage, which is spherical and radial. The existence of siderite has a positive catalytic effect on the pyrolysis of organic matter and the generation of hydrocarbons.

5.1.2 Paleoclimate Analysis

Paleoclimate change restricts the population density and biological assemblage in the water body by affecting the sediment supply and water stratification. It also indirectly affects the enrichment and preservation of organic matter. Previous studies have shown that the relative content of some trace elements in mud shale can indicate the paleoclimate and the depositional environment at that time (Yang et al., 2009). Among them, the ratio of element Sr to

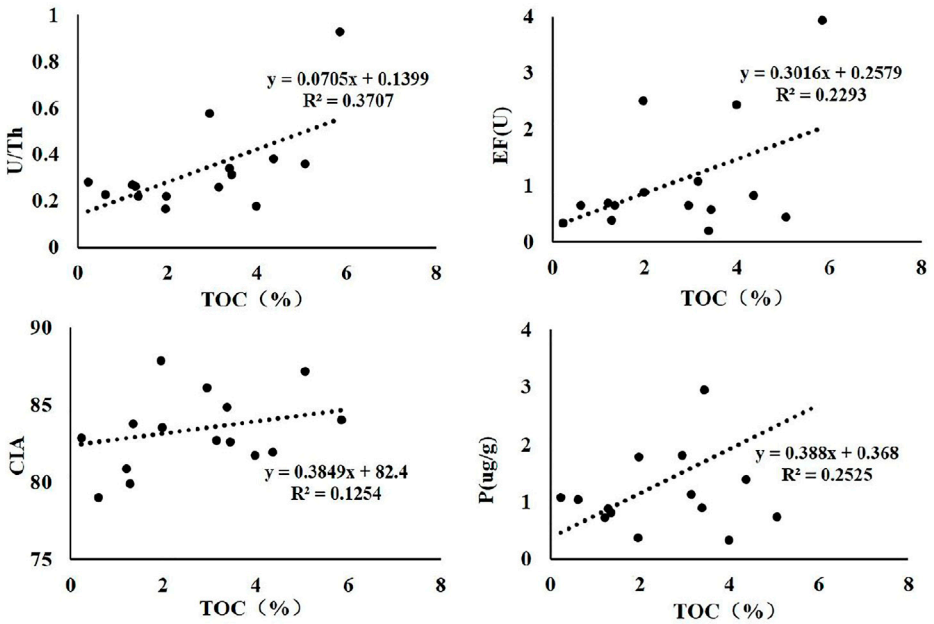

FIGURE 9 | Correlations between TOC and redox properties, paleoproductivity, and paleoclimate indicators of Longtan Formation shale in Well X1 in the study area.

element Cu is very sensitive to changes in the paleoclimate. Large Sr/Cu indicates a hot and dry climate, and small Sr/Cu indicates a warm and humid climate. It is generally believed that a Sr/Cu ratio of 1.30:5.00 suggests a warm and humid climate, and a Sr/Cu ratio greater than 5.00 suggests a dry and hot climate (Leman, 1984). The Sr/Cu ratio in the study area was 0.75:5.72, with an average value of 2.90 (**Figure 8**), indicating that the climate during the deposition of the Longtan Formation was warm and humid.

In addition to evaluating the degree of chemical weathering, the Chemical Index of Alteration (CIA) is also widely utilized to evaluate paleoclimate changes. In this study, the CIA proposed by Nesbitt and Young (1982) was employed to evaluate the paleoclimate conditions during the sedimentary period of marine-continental transitional facies shale of the Lower Longtan Formation (Nesbitt and Young, 1982). The calculation formula is as follows:

$$CIA = \left[\frac{Al_2O_3}{CaO^* + Al_2O_3 + Na_2O + K_2O}\right] \times 100$$

In the above formula, all oxide units are in the molar system, and CaO* refers only to CaO in silicate minerals. Since there was no good method to directly determine the relative contents of non-silicate minerals and silicate minerals in the sample, we used the P_2O_5 content to indirectly calculate them (Ding et al., 2021). The used formula is as follows:

$$CaO^* = CaO - P_2O_5 \times 10/3$$

When m (Na_2O) ≤ m(CaO*), then m(CaO*) = m(Na_2O). In contrast, when m (Na_2O) > m(CaO*), m(CaO*) = m(CaO). The m refers to the number of moles of oxide.

In general, large CIA values indicate warm and humid paleoclimates, while small CIA values reflect dry and cold paleoclimates. In particular, when the CIA is between 50 and 65, it reflects a dry-cool climate with weak chemical weathering. When the CIA is between 65 and 80, it reflects a warm and humid climate with moderate chemical weathering. When the CIA is between 80 and 100, it reflects a hot-humid climate with strong chemical weathering (Ding et al., 2021; Bai et al., 2015). The CIA of the Longtan Formation shale samples in the study area was between 79 and 87.85, with an average value of 83.26, and a CIA of 65–85 accounted for 70% of the data (**Table 2**; **Figure 8**), indicating that the climate during the deposition of the Longtan Formation was warm and humid.

5.1.3 Influencing Factors of Organic Matter Enrichment

According to the ratio of the evaluation index $(La/Yb)_N$ (UCC standardization) of the rare earth element distribution model, the ratio of mud shale samples of the Longtan Formation in Well X1 in the study area $(La/Yb)_N$ was distributed in the range of 4.04–18.89, with an average value of 10.52. This is significantly greater than 1.0, indicating that the deposition rate at that time was small (**Figure 8**). From the above analysis, it can be observed that the sea-land transitional shale in the Longtan Formation of Well X1 in the study area was in a warm-humid climate during the deposition period. The main body of the sedimentary water is in an oxygen-poor environment, and it is in an oxidized state during some periods. It has high bio-paleoproductivity and a small deposition rate. TOC is the most intuitive indicator of the degree of organic matter enrichment. By counting the correlation between TOC and U/Th, EF (U), CIA, and P element content, we

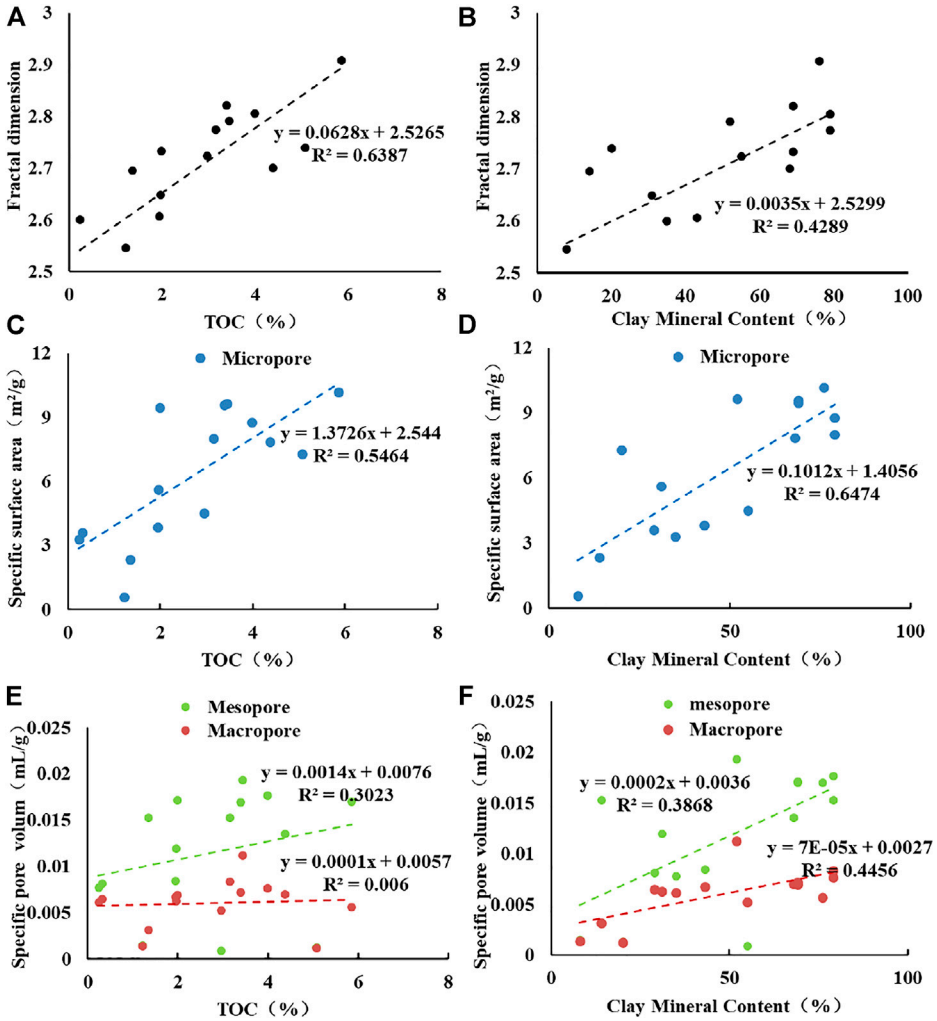

FIGURE 10 | Relationship between organic carbon content, clay mineral content, and pore structure characteristic parameters. **(A)** The relationship between organic carbon and fractal dimension. **(B)** The relationship between clay minerals and the fractal dimension. **(C)** The relationship between organic carbon and specific surface area. **(D)** The relationship between clay minerals and specific surface area. **(E)** The relationship between organic carbon and specific pore volume. **(F)** The relationship between clay minerals and specific pore volume.

observe from **Figure 9** that the correlation between them is not very obvious (R^2 = 0.3707, 0.2293, 0.1254, 0.2525). That is, different from the enrichment law of organic matter in marine shale, the formation and enrichment of organic matter in the transitional facies of the Longtan Formation in Well X1 are not determined by a single factor. This is the result of the mutual configuration and coupling of multiple elements such as paleoclimate, water redox properties, paleoproductivity, and depositional environment. These factors will directly or indirectly affect the supply of organic matter or the burial and preservation of organic matter in the mud shale of the Longtan Formation in the study area. Under the condition of high biological productivity, the temperature and humidity environment of the mud shale of the Longtan Formation in Well X1 is conducive to the flourishing of organisms and the formation of organic matter. However, due to the small deposition rate and the oxygen-containing environment, some organic matter is decomposed in the water body, and the preservation and enrichment of organic matter are limited to a certain extent.

5.2 Influencing Factors of Reservoir Development

In shale reservoirs, factors such as sedimentary facies, organic matter content, and mineral composition jointly control the storage space, natural gas occurrence state, and shale gas enrichment degree (Zhao et al., 2020; Wang et al., 2020; Ma et al., 2021; Zhang et al., 2020c; Zhang et al., 2022d). The results of the liquid nitrogen adsorption–desorption test showed that the distribution of characteristic parameters of pore structure in different samples was significantly different. Different mineral

compositions in shale reservoirs control the development of reservoir space and have different degrees of influence on the development of reservoir space (Zhang et al., 2020d; Zhang et al., 2022e). **Figures 10A,B** shows that the organic carbon content, clay mineral content, and the pore structure fractal dimension D have a certain positive correlation. The correlation coefficient (R^2) between the organic carbon content and the pore structure fractal dimension D is 0.6387, and R^2 between the clay mineral content and D is 0.4289. The reservoir space in the samples was mainly developed in organic matter and clay minerals. The increase in organic carbon content and clay mineral content boosts the heterogeneity of the pore structure of mud shale and the roughness of the surface of the storage space, which can provide more adsorption sites and storage space for the occurrence of shale gas.

The organic carbon content and clay mineral content of different shale test samples in Well X1 were positively correlated with the specific surface area of micropores. R^2 between the organic carbon content and clay mineral content with the specific surface area of micropores is 0.5464 and 0.6474. The relationship with the specific surface area of mesopores and macropores was not obvious; all the correlation coefficients are less than 0.5 (**Figures 10C–F**). The sedimentary environment of the Longtan Formation in the study area is a marine-continental transitional facies environment. During the deposition period, it was in a warm and humid climate, and the sedimentary water was in an oxygen-deficient state, accompanied by an oxidation state, with high biological productivity. The smaller deposition rate and the oxygen-rich environment allow some of the organic matter to be decomposed in the water body. Microscopic observations showed the development of organic pores and organic margins. Moreover, the content of clay minerals in the samples was high, mainly chlorite and a mixed layer of illite/smectite. Because of the fine particle size of layered silicate minerals, lamellar illite/smectite mixed beds and chlorite aggregates often develop interlayer pores or microfractures. Both contribute positively to the pore volume size of the sample.

6 CONCLUSION

(1) The Longtan Formation in the study area belongs to the marine-continental transitional facies and mainly develops delta and tidal flat-lagoon sedimentary systems. The lithology is complex, mainly composed of thick mud shale interbedded with limestone, siltstone, and interbedded mud shale, siltstone, and limestone, as well as coal seam/coal line interbedding. The kerogen types of the samples were mainly II_1 and II_2-III, the main microscopic components were chitinite and vitrinite, and the TOC was mostly distributed between 2.0%–3.0% and 4.0%–5.0%. The average maturity was 3.11%, which was in the high maturity stage. The storage space of the reservoir included inorganic pores, organic pores, and microfractures. The difference in the "hysteresis loop" in the liquid nitrogen adsorption and desorption test results indicated that there were two different forms of storage space. Micropores were almost developed, which mainly contributed to the specific surface area of the samples, and the volume of mesopores was the main contribution to the relative pore volume, followed by macropores.

(2) Through the index values of V/Cr, U/T, enrichment coefficients EF (Mo) and EF (U), chemical alteration indexes CIA and Sr/Cu, and Mo, P, and other index values of different samples, the depositional environment of the Longtan Formation in the study area was systematically analyzed. The Longtan Formation was in a warm and humid climate during the depositional period. The main body of the sedimentary water was in an oxygen-depleted state, and part of it was in an oxidized state. It had high biological productivity and a small deposition rate. The formation and enrichment of organic matter in the shale of the sea-land transitional facies in the Longtan Formation in Well X1 could not be determined by a single factor. Under the condition of high biological productivity, the warm and humid environment is conducive to the flourishing of organisms and the formation of organic matter, but the smaller deposition rate and the oxygen-containing environment cause some organic matter to be decomposed in the water body, and the preservation and enrichment of organic matter are limited to a certain extent.

(3) The content of clay minerals and organic matter in shale samples played a major role in controlling the development of reservoir space. The content of TOC and clay minerals were positively correlated with the specific surface area of micropores and the specific pore volume of mesopores. The content of organic matter in the test samples of the Longtan Formation in the study area was high, and the mineral components were chiefly clay minerals such as chlorite and a mixed layer of illite/smectite. Microscopic observation suggested that organic matter pores and organic matter edges were developed, and interlayer pores or microfractures were often found in lamellar illite/smectite mixed layer and chlorite aggregates, which played a positive role in the specific surface area and pore volume of the samples.

DATA AVAILABILITY STATEMENT

The original contributions presented in the study are included in the article/Supplementary Material; further inquiries can be directed to the corresponding author.

AUTHOR CONTRIBUTIONS

QC and MQ conceived and designed the experiments and wrote the manuscript; QC, XL, and YD performed the experiments and wrote the manuscript; QC and DW analyzed the data; DW and CW revised the manuscript and provided language support; MQ and YD provided technical support.

ACKNOWLEDGMENTS

We sincerely appreciate all reviewers and the handling editor for their critical comments and constructive suggestions.

REFERENCES

Arthur, M., and Sageman, B. (1994). Marine Black Shales: Depositional Mechanisms and Environments of Ancient Deposits. *Annu. Rev. Earth Planet. Sci.* 22, 499–551. doi:10.1146/annurev.ea.22.050194.002435

Bai, Y., Liu, Z., Sun, P., Liu, R., Hu, X., Zhao, H., et al. (2015). Rare Earth and Major Element Geochemistry of Eocene Fine-Grained Sediments in Oil Shale- and Coal-Bearing Layers of the Meihe Basin, Northeast China. *J. Asian Earth Sci.* 97, 89–101. doi:10.1016/j.jseaes.2014.10.008

Cai, J., Bao, Y., Yang, S., Wang, X., Fan, D., Xu, J., et al. (2007). Research on Preservation and Enrichment Mechanisms of Organic Matter in Muddy Sediment and Mudstone. *Sci. China Ser. D-Earth Sci.* 50, 765–775. doi:10.1007/s11430-007-0005-0

Cao, Q., Zhou, W., Deng, H., and Chen, W. (2015). Classification and Controlling Factors of Organic Pores in Continental Shale Gas Reservoirs Based on Laboratory Experimental Results. *J. Nat. Gas Sci. Eng.* 27, 1381–1388. doi:10.1016/j.jngse.2015.10.001

Chang, H., Chu, X., Feng, L., Huang, J., and Zhang, Q. (2009). Redox Sensitive Trace Elements as Paleoenvironments Proxies. *Geol. Rev.* 55, 91–99 (In Chinese). doi:10.1016/S1874-8651(10)60080-4

Chen, F., Wei, X., Liu, Z., Ao, M., and Yan, J. (2020). Pore Development Characteristics and Main Controlling Factors of the Permian Marine-Continent Transitional Shale in the Sichuan Basin. *Nat. Gas. Geosci.* 31, 1593–1602. (In Chinese). doi:10.11764/j.issn.1672-1926.2020.04.028

Cheng, F., Wei, X., Liu, Z., Ao, M., and Yan, J. (2020). Pore Development Characteristics and Main Controlling Factors of the Permian Marine-Continent Transitional Shale in the Sichuan Basin. *Nat. Gas. Geosci.* 31, 1593–1602. (In Chinese). doi:10.11764/j.issn.1672-1926.2020.04.028

Demaison, G., and Moore, G. (1980). Anoxic Environments and Oil Source Bed Genesis. *AAPG Bull.* 64, 1179–1209. doi:10.1306/2f91945e-16ce-11d7-8645000102c1865d

Ding, J., Zhang, J., Shi, G., Shen, B., and Tang, X. (2021). Sedimentary Environment and Organic Matter Enrichment Mechanisms of the Upper Permian Dalong Formation Shale, Southern Anhui Province, China. *Oil Gas. Geol.* 42, 158–172. (In Chinese). doi:10.11743/ogg20210114

Dong, D., Wang, Y., Li, X., and Zou, C. (2016). Breakthrough and Prospect of Shale Gas Exploration and Development in China. *Nat. Gas. Ind.* 36, 19–32. (In Chinese). doi:10.1016/j.ngib.2016.02.002

Guo, X., Hu, D., Liu, R., Wei, X., and Wei, F. (2018). Geological Conditions and Exploration Potential of Permian Marine–Continent Transitional Facies Shale Gas in the Sichuan Basin. *Geol. Prospect.* 38, 11–18 (In Chinese). doi:10.3787/j.issn.1000-0976.2018.10.002

Hatch, J., and Leventhal, J. (1992). Relationship between Inferred Redox Potential of the Depositional Environment and Geochemistry of the Upper Pennsylvanian (Missourian) Stark Shale Member of the Dennis Limestone, Wabaunsee County, Kansas, U.S.A. *Chem. Geol.* 99 (1–3), 65–82. doi:10.1016/0009-2541(92)90031-y

He, Y., Tang, X., Shan, Y., Liu, G., Xie, H., and Ma, Z. (2021a). Lithofacies Division and Comparison and Characteristics of Longtan Formation Shale in Typical Areas of Sichuan Basin and its Surrounding. *Nat. Gas. Geosci.* 32, 174–190. (In Chinese)). doi:10.11764/j.issn.1672-1926.2020.09.009

He, Y., Nie, H., Li, S., Liu, G., and Ding, J. (2021b). Differential Occurence of Shale Gas in the Permian Longtan Formation of Upper Yangtze Region Constrained by Plate Tectonics in the Tethyan Domain. *Oil Gas Geol* 42, 1–15 (In Chinese). doi:10.11743/ogg20210101

Huang, Z., Wang, X., Yang, X., Zhu, R., Cui, J., Lu, Y., et al. (2021). Constraints of Sedimentary Environment on Organic Matter Accumulation in Shale: A Case Study of the Wufeng-Longmaxi Formations in the Southern Sichuan Basin. *Acta Sedimentol. Sin.* 39, 631–644 (In Chinese). doi:10.14027/j.issn.1000-0550.2020.120

IUPAC (1982). Reporting Physisorption Data for Gas/solid Systems with Special Reference to the Determination of Surface Area and Porosity. *Pure Appl. Chem.* 54, 2201–2218. doi:10.1351/pac198557040603

Leman, M. (1984). Factors Controlling the Proportionality of Vanadium to Nickel in Crude Oils. *Geochimica Cosmochimica Acta* 48, 2231–2238. doi:10.1016/0016-7037(84)90219-9

Liu, Z., Li, S., Xin, R., Xu, C., and Cheng, J. (2007). Paleoclimatic Information in Stratigraphic Records and its Relation to the Formation of Hydrocarbon Source Rocks-A Case Study of the Paleogene Strata in the Huanghekou Subbasin of the Bohai Bay Basin, China. *Geol. Bull. China* 26, 830–840. (In Chinese). doi:10.3969/j.issn.1671-2552.2007.07.006

Ma, R., Zhang, J., Wang, M., Ma, W., and Zhao, J. (2021). Micro-pore Characteristics and Gas- Bearinies Property of Marine Continental Transitional Shale Reservoirs in the Qinshui Basin. *J. Henan Polytech. Univ. Nat. Sci.* 40, 66–77 (In Chinese). doi:10.16186/j.cnki.1673-9787.2019120015

Nesbitt, H., and Young, G. (1982). Early Proterozoic Climates and Plate Motions Inferred from Major Element Chemistry of Lutites. *Nature* 299, 715–717. doi:10.1038/299715a0

Pedersen, T., and Calvert, S. (1990). Anoxia vs. Productivity: What Controls the Formation of Organic-Carbon-Rich Sediments and Sedimentary Rocks? *AAPG Bull.* 74, 454–466. doi:10.1306/0c9b232b-1710-11d7-8645000102c1865d

Taylor, S., and McLennan, S. (1985). The Continental Crust: its Composition and Evolution. *J. Geol.* 94, 57–72.

Tribovillard, N., Algeo, T. J., Lyons, T., and Riboulleau, A. (2006). Trace Metals as Paleoredox and Paleoproductivity Proxies: An Update. *Chem. Geol.* 232, 12–32. doi:10.1016/j.chemgeo.2006.02.012

Tribovillard, N., Algeo, T. J., Baudin, F., and Riboulleau, A. (2012a). Analysis of Marine Environmental Conditions Based Onmolybdenum-Uranium Covariation-Applications to Mesozoic Paleoceanography. *Chem. Geol.* 324-325 (none), 46–58. doi:10.1016/j.chemgeo.2011.09.009

Tribovillard, N., Bout-Roumazeilles, V., Algeo, T., Lyons, T. W., Sionneau, T., Montero-Serrano, J. C., et al. (2012b). Paleodepositional Conditions in the Orca Basin as Inferred from Organic Matter and Trace Metal Contents. *Mar. Geol.* 254 (1), 62–72. doi:10.1016/j.margeo.2008.04.016

Wang, W., Shi, W., Fu, X., and Chen, C. (2020). Shale Gas Exploration Potential and Target of Permian Dalong Formation in Northern Sichuan. *Coal Geol. China* 42, 892–899. (In Chinese). doi:10.11781/sysydz202006892

Wedepohl, K. H. (1971). Environmental Influences on the Chemical Composition of Shales and Clays. *Phys. Chem. Earth* 8, 307–333. doi:10.1016/0079-1946(71)90020-6

Wei, H., Chen, D., Wang, J., Yu, H., and Tucker, M. E. (2012). Organic Accumulation in the Lower Chihsia Formation (Middle Permian) of South China: Constraints from Pyrite Morphology and Multiple Geochemical Proxies. *Palaeogeogr. Palaeoclimatol. Palaeoecol.* 353-355, 73–86. doi:10.1016/j.palaeo.2012.07.005

Wei, Z., Wang, Y., Wu, C., Wu, B., Sun, Z., Li, S., et al. (2015). Geochemical Characteristics of Source Rock from Upper Permian Longtan Formation in Sichuan Basin. *Nat. Gas. Geosci.* 26, 1613. (In Chinese). doi:10.11764/j.issn.1672-1926.2015.08.1613

Wignall, P. B., and Newton, R. (2001). Black Shales on the Basin Margin: a Model Based on Examples from the Upper Jurassic of the Boulonnais, Northern France. *Sediment. Geol.* 144, 335–356. doi:10.1016/s0037-0738(01)00125-7

Yang, X., Zhang, L., Li, J., and Wu, J. (2009). Characteristics of Micro-pore Structure in Sulige Gasfield in Ordos Basin. *Geol. Sci. Technol. Inf.* 28, 73–76 (In Chinese). doi:10.3969/j.issn.1000-7849.2009.03.013

Yang, X., Fang, K., Luo, P., Zhao, S., and Ye, D. (2021). Shale Gas Exploration Potential and Target of Permian Dalong Formation in Northern Sichuan. *Sediment. Geol. Tethyan Geol.* 41, 446–453 (In Chinese). doi:10.19826/j.cnki.1009-3850.2021.06005

Yin, J., Yu, Y., Jiang, C., Liu, J., Zhao, Q., and Shi, P. (2017). Relationship between Element Geochemical Characteristic and Organic Matter Enrichment in Zhangjiatan Shale of Yanchang Formation, Ordos Basin. *J. China Coal Soc.* 42, 1544–1556. (In Chinese). doi:10.13225/j.cnki.jccs.2016.1342

Zhang, J., Li, Q., and Liu, Y. (2014). Longtan Formation Shale Gas Reservoiring Conditions and Favorable Region Analysis in Southern Sichuan Area. *Coal Geol. China* 26, 6 (In Chinese). doi:10.3969/j.issn.1674-1803.2014.12.01

Zhang, J., Li, Q., Guo, M., Dong, Z., Wang, Z., Fu, Q., et al. (2015). Microscopic Pore Characteristics and its Influence Factors of the Permian Longtan Formation Shales in the Southern Sichuan Basin. *Nat. Gas. Geosci.* 26, 1571–1578 (In Chinese).

Zhang, P., Huang, Y., Zhang, J., Liu, H., and Yang, j. (2018). Fractal Characteristics of the Longtan Formation Transitional Shale in Northwest Guizhou. *J. China Coal Soc.* 43, 6 (in Chinese). doi:10.13225/j.cnki.jccs.2018.4046

Zhang, K., Peng, J., Liu, W., Li, B., Xia, Q., Cheng, S., et al. (2020a). The Role of Deep Geofluids in the Enrichment of Sedimentary Organic Matter: A Case Study of the Late Ordovician-Early Silurian in the Upper Yangtze Region and Early Cambrian in the Lower Yangtze Region, South China. *Geofluids* 2020, 1–12. doi:10.1155/2020/8868638

Zhang, K., Peng, J., Wang, X., Jiang, Z., Song, Y., Jiang, L., et al. (2020b). Effect of Organic Maturity on Shale Gas Genesis and Pores Development: A Case Study on Marine Shale in the Upper Yangtze Region, South China. *Open Geosci.* 12, 1617–1629. doi:10.1515/geo-2020-0216

Zhang, K., Jia, C., Song, Y., Jiang, S., Jiang, Z., Wen, M., et al. (2020c). Analysis of Lower Cambrian Shale Gas Composition, Source and Accumulation Pattern in Different Tectonic Backgrounds: A Case Study of Weiyuan Block in the Upper Yangtze Region and Xiuwu Basin in the Lower Yangtze Region. *Fuel* 263, 115978. doi:10.1016/j.fuel.2019.115978

Zhang, X., Li, X., Li, Y., He, Y., and Zhang, J. (2020d). Research Progress of Reservoir of Shale Gas in Coal Measures. *Coal Geol. China* 32, 59–66 (In Chinese). doi:10.3969/j.issn.1674-1803.2020.02.12

Zhang, K., Jiang, Z., Song, Y., Jia, C., Yuan, X., Wang, X., et al. (2022a). Quantitative Characterization for Pore Connectivity, Pore Wettability, and Shale Oil Mobility of Terrestrial Shale with Different Lithofacies-A Case Study of the Jurassic Lianggaoshan Formation in the Southeast Sichuan Basin of the Upper Yangtze Region in Southern China. *Front. Earth Sci.* 10, 864189. doi:10.3389/feart.2022.864189

Zhang, K., Song, Y., Jiang, Z., Xu, D., Li, L., Yuan, X., et al. (2022b). Quantitative Comparison of Genesis and Pore Structure Characteristics of Siliceous Minerals in Marine Shale with Different TOC Contents-A Case Study on the Shale of Lower Silurian Longmaxi Formation in Sichuan Basin, Southern China. *Front. Earth Sci.* 10, 887160. doi:10.3389/feart.2022.887160

Zhang, K., Jiang, S., Zhao, R., Wang, P., Jia, C., and Song, Y. (2022c). Connectivity of Organic Matter Pores in the Lower Silurian Longmaxi Formation Shale, Sichuan Basin, Southern China: Analyses from Helium Ion Microscope and Focused Ion Beam Scanning Electron Microscope. *Geol. J.* 57 (5), 1912–1924. doi:10.1002/gj.4387

Zhang, K., Song, Y., Jia, C., Jiang, Z., Han, F., Wang, P., et al. (2022d). Formation Mechanism of the Sealing Capacity of the Roof and Floor Strata of Marine Organic-Rich Shale and Shale Itself, and its Influence on the Characteristics of Shale Gas and Organic Matter Pore Development. *Mar. Petroleum Geol.* 140, 105647. doi:10.1016/j.marpetgeo.2022.105647

Zhang, Q., Qiu, Z., Zhao, Q., Zhang, L., Dong, D., Wang, Y., et al. (2022e). Composition Effect on the Pore Structure of Transitional Shale: A Case Study of the Permian Shanxi Formation in the Daning-Jixian Block at the Eastern Margin of the Ordos Basin. *Front. Earth Sci.* 9, 802713. doi:10.3389/feart.2021.802713

Zhao, P., Gao, B., Guo, Z., and Wei, Z. (2020). Exploration Potential of Marine-Continental Transitional and Deep-Water Shelf Shale Gas in Upper Permian, Sichuan Basin. *Pet. Geol. Exp.* 42, 335–344. (In Chinese).

Zhu, Z., Chen, H., Lin, L., Hou, M., Chen, A., and Zhong, Y. (2010). Depositional System Evolution Characteristics in the Framework of Sequences of Silurian and Prediction of Favorable Zones in the Northern Guizhou-Southeastern Sichuan. *Acta Sedimentol. Sin.* 28, 243–253. (In Chinese).

Conflict of Interest: The authors declare that the research was conducted in the absence of any commercial or financial relationships that could be construed as a potential conflict of interest.